Taylor & Francis
Taylor & Francis Group

Just Accepted by *Nanotoxicology*

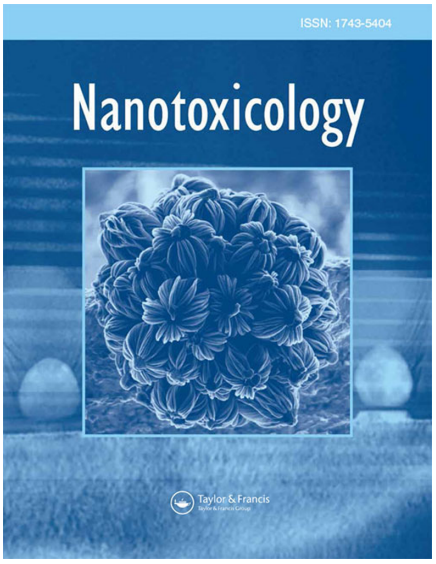

Food web effects of titanium dioxide nanoparticles in an outdoor freshwater mesocosm experiment

Boris Jovanović, Gizem Bezirci, Ali Serhan Çağan, Jan Coppens, Eti E. Levi, Zehra Oluz, Eylül Tuncel, Hatice Duran, Meryem Beklioğlu

Doi: 10.3109/17435390.2016.1140242

Abstract

Over the course of 78 days, 9 outdoor mesocosms, each with 1350 L capacity, were situated on a pontoon platform in the middle of a lake and exposed to 0 µg L^{-1} TiO_2, 25 µg L^{-1} TiO_2, or 250 µg L^{-1} TiO_2 nanoparticles in the form of E171 TiO_2 human food additive five times a week. Mesocosms were inoculated with sediment, phytoplankton, zooplankton, macroinvertebrates, macrophytes, and fish before exposure, ensuring a complete food web. Physicochemical parameters of the water, nutrient concentrations, and biomass of the taxa were monitored. Concentrations of 25 µg L^{-1} TiO_2 and 250 µg L^{-1} TiO_2 caused a reduction in available soluble reactive phosphorus in the mesocosms by 15% and 23%, respectively, but not in the amount of total phosphorous. The biomass of Rotifera was significantly reduced by 32% and 57% in the TiO_2 25 µg L^{-1} and TiO_2 250 µg L^{-1} treatments, respectively, when compared to the control; however, the biomass of the other monitored groups—Cladocera, Copepoda, phytoplankton, macrophytes, chironomids, and fish—remained unaffected. In conclusion, environmentally relevant concentrations of TiO_2 nanoparticles may negatively affect certain parameters and taxa of the freshwater lentic aquatic ecosystem. However, these negative effects are not significant enough to affect the overall function of the ecosystem, as there were no cascade effects leading to a major change in its trophic state or primary production.

Food web effects of titanium dioxide nanoparticles in an outdoor freshwater mesocosm experiment

Boris Jovanović [a,b*], Gizem Bezirci[c], Ali Serhan Çağan[c], Jan Coppens[c], Eti E. Levi[c], Zehra Oluz[d], Eylül Tuncel[d], Hatice Duran[d], Meryem Beklioğlu[c,e]

[a]*Chair for Fish Diseases and Fisheries Biology, Faculty of Veterinary Medicine, Ludwig Maximilian University of Munich (LMU), Munich, Germany*

[b]*Center for Nanoscience (CeNS), LMU, Munich, Germany*

[c]*Department of Biology, Middle East Technical University, Ankara, Turkey*

[d]*Department of Materials Science and Nanotechnology Engineering, TOBB University of Economics and Technology, Ankara, Turkey*

[e]*Kemal Kurdaş Ecological Research and Training Stations, Lake Eymir, Middle East Technical University, Ankara, Turkey*

[*] Corresponding author:
Boris Jovanović
Chair for Fisheries Biology and Fish Diseases
Department of Veterinary Sciences
Faculty of Veterinary Medicine
Ludwig Maximilian University of Munich
Kaulbachstrasse 37, 80539 Munich, Germany
nanoaquatox@gmail.com

Abstract

Over the course of 78 days, 9 outdoor mesocosms, each with 1350 L capacity, were situated on a pontoon platform in the middle of a lake and exposed to 0 µg L^{-1} TiO_2, 25 µg L^{-1} TiO_2, or 250 µg L^{-1} TiO_2 nanoparticles in the form of E171 TiO_2 human food additive five times a week. Mesocosms were inoculated with sediment, phytoplankton, zooplankton, macroinvertebrates, macrophytes, and fish before exposure, ensuring a complete food web. Physicochemical parameters of the water, nutrient concentrations, and biomass of the taxa were monitored. Concentrations of 25 µg L^{-1} TiO_2 and 250 µg L^{-1} TiO_2 caused a reduction in available soluble reactive phosphorus in the mesocosms by 15% and 23%, respectively, but not in the amount of total phosphorous. The biomass of Rotifera was significantly reduced by 32% and 57% in the TiO_2 25 µg L^{-1} and TiO_2 250 µg L^{-1} treatments, respectively, when compared to the control; however, the biomass of the other monitored groups—Cladocera, Copepoda, phytoplankton, macrophytes, chironomids, and fish—remained unaffected. In conclusion, environmentally relevant concentrations of TiO_2 nanoparticles may negatively affect certain parameters and taxa of the freshwater lentic aquatic ecosystem. However, these negative effects are not significant enough to affect the overall function of the ecosystem, as there were no cascade effects leading to a major change in its trophic state or primary production.

Keywords: E171, titanium dioxide, plankton, mesocosms, environmental toxicology

Introduction

The application of emerging nanotechnology in various fields is releasing nanoparticles into the environment at an increasing pace. Therefore, ecotoxicological findings are needed in order to carry out adequate risk assessment. Risk assessment is currently governed by European Government and Council regulations concerning REACH: the Registration, Evaluation, Authorization, and Restriction of Chemicals (European Parliament, 2006). Recent legislation has further clarified how REACH applies to nanomaterials (European Commission, 2008). In 2006, the Chemicals Committee of the Organization for Economic Co-operation and Development (OECD) formed a special Working Party on Manufactured Nanomaterials (WPMN). Its purpose was to examine the potential impact of nanoparticles on the environment and on human health, focusing predominantly on testing and assessment methods. In 2007, the WPMN launched a special program and agreed on a priority list of nanomaterials and relevant endpoints for environmental safety testing. One of the nanomaterials in the OECD WPMN priority list is titanium dioxide (TiO_2).

Between 1916 and 2011, an estimated total of 165,050,000 metric tonnes of TiO_2 was produced worldwide, including both nano and bulk forms (Jovanović, 2015a). Nano-TiO_2 is used as a constituent in sunscreens, soaps, shampoos, toothpastes, and other cosmetics, as well as in the paper, building materials, plastics, ink, pharmaceuticals, and food industries. As a colorant ingredient in food products, TiO_2 is often listed as E171 and used in a variety of common food products, with an estimated human consumption of 1 mg kg^{-1} body weight per day (Weir et al., 2012). E171 is a European Union designation for a white food color additive known elsewhere by designations such as CI77891 or Pigment White 6. A significant portion of TiO_2 in E171 is in the nano-form (Weir et al., 2012; Yang et al., 2014).

The estimated environmental concentration of nano-TiO_2 in surface water is 0.7 to 16 µg L^{-1} (Mueller and Nowack, 2008); in the case of treated wastewater, effluent concentration is around 25 µg L^{-1} (Westerhoff et al., 2011). In urban runoff, concentration can be as high as 600 µg L^{-1} (Kaegi et al.,

2008), and in the case of raw sewage, up to 3000 µg L^{-1} (Kiser et al., 2009; Westerhoff et al., 2011). Recently, it was suggested that a major source of nano-TiO_2 in the environment may in fact be E171, rather than coming from textile or other industry emissions (Windler et al., 2012). In a large European coastal metropolis such as Istanbul, which has 14 million people, the daily excretory contribution of both nano, micro, and bulk TiO_2 to municipal wastewater via raw sewage would be 980 kg (roughly 1 tonne), as on average a person consumes approximately 70 mg of TiO_2 per day or 1 mg/kg body weight (Weir et al., 2012). It has been estimated that 96% of all TiO_2 is removed from raw sewage in wastewater treatment plants, but the remaining 4% is released to the aquatic environment (Westerhoff et al., 2011) predominantly in the nano size. In the case of Istanbul, this dispersal would result in an approximate discharge of 40 kg of TiO_2 per day (almost 15 tonnes per year) into the aquatic environment in the form of E171 TiO_2 food color alone. A significant portion of these 15 tonnes may be in nano-form, since smaller particles pass through filters more easily. Concentration of TiO_2 in wastewaters from production and refinement factories are even higher, in the range of 1 g L^{-1}. For example, the concentration of TiO_2 in the wastewater supernatant of the TiO_2 producing factory in Finland was determined to be 1.3 g L^{-1} (Lehtinen et al., 1984). However, no information was provided on particle size.

So far, other than standard toxicity texts, very little data have been acquired about the potential impacts of TiO_2 on the ecosystem (either nano or microsized), rather than on a species or population. Furthermore, existing data often conflict. For example, the addition of TiO_2 nanoparticles to algae culture medium directly increases the biomass of many freshwater algae species (Kulacki and Cardinale, 2012). Inversely, nano and micro TiO_2 is photo sensitive and can express bactericidal and algaecidal effects by producing reactive oxygen species (Cheng et al., 2008; Coleman et al., 2005; Huang et al., 2000; Miller et al., 2012). TiO_2 nanoparticles can also affect the oxidation rate of ammonia, promoting its conversion to non-toxic form and thus potentially playing an important role in the reduction of eutrophication (Altomare and Selli, 2013). Nano-TiO_2 impacts the pore water surface

properties of freshwater sediments and increases sediment phosphorus adsorption capacity to its maximum (Luo et al., 2011). Similarly, among all of the tested nanomaterials, TiO_2 has the highest removal rate of phosphorous in water, with an adsorption coefficient of 28.3 mg g^{-1}, and the lowest desorption capacity; thus, it could potentially be used for controlling and preventing eutrophication (Moharami and Jalali, 2014). Nano-TiO_2 retains phosphorous impurities from its production process (Liu et al., 2013; Yang et al., 2014), delivering extra phosphorus to aquatic ecosystems. In a study conducted with hydroponic tomatoes, it was concluded that titanium (Ti) may compensate for nitrogen (N) deficiencies on plant growth and metabolism, probably because Ti enhances both the bioavailability of N and the N root uptake in these terrestrial plants (Haghighi et al., 2012). However, it is unknown whether nano-TiO_2 can exert any similar effects on macrophytes. In fact, a standard OECD No. 221 toxicity test demonstrated that nano-TiO_2 can inhibit the growth of duckweed (Lemna sp.) with a lowest observed effect concentration of 125 ppm (Kim et al., 2011). Furthermore, long-term exposure of wastewater-activated sludge to nano-TiO_2 can significantly reduce total nitrogen (TN) removal efficiency and reduce diversity of the microbial community (Zheng et al., 2011). It is unclear whether this effect can be manifested in an aquatic ecosystem.

Despite such conflicting reports, some progress has been made with higher tier toxicity testing. For example, a study performed in a paddy microcosm showed that nano-TiO_2 had bioaccumulated in hydrobiota and was transferred from prey (biofilm, water dropwort) to predator (nematodes and mudsnails) in a trophic food chain (Yeo and Nam, 2013). However, this experiment was oversimplified, short (17 days), and without many of the recommended OECD monitoring endpoints (OECD, 2006), thus reducing the relevance of conclusions other than the effects of bioaccumulation and trophic transfer. In another study, microcosms were again employed to study the effect of nano-TiO_2 bioaccumulation in aquatic organisms (Kulacki et al., 2012). Results were similar to the previous study, showing nano-TiO_2 accrual in biofilms and bioaccumulation in freshwater snails after the consumption of biofilms.

Still, no studies have examined the effects of TiO_2 (nano or micro) from the food web perspective in an outdoor freshwater mesocosm experiment set up according to OECD guidelines for higher tier testing. This paper aims to fill this major gap by investigating the following hypothesis: Exposure of lentic freshwater mesocosms to E171 TiO_2 will cause measurable changes in biomass production, from primary producers to zooplankton and invertebrates, through changes in availability of phosphorous, nitrogen, and sunlight.

Methodology

Mesocosms setup

The experiment was conducted in METU Golet (39° 52′ 11″ N, 32° 46′ 29″ E), a small lake belonging to Middle East Technical University of Ankara, Turkey. The area of the lake is 2 ha, with a maximum depth of 11 m. It is situated 998 m above sea level, is surrounded by hills and forest, and does not receive any municipal waste water. Swimming and other outdoor activities are forbidden. The general public, outside of university personnel, is not allowed to visit, and the experimental area is guarded 24 hours per day.

Setup included a floating pontoon platform for storing all mesocosms together (Supporting Figure S1). It held 9 identical cylindrical (1.2 m D) fiberglass (4 mm thick) tanks (1.2 m high), as described in our previous study (Landkildehus et al., 2014). The platform was anchored in the middle of the lake. After anchoring, 0.113 m^3 of lake sediment (10 cm of the tank height) was added to each mesocosm. The sediment was dug from the lake with a shovel, sieved through 1 cm^2 mesh, and dried by exposure to sunlight for one week to prevent the hatching of any fish eggs. Following sediment addition, the mesocosms were filled with 500 µm filtered lake water (1100 L each). The nutrient concentration of the lake water at the time was 0.045 mg L^{-1} of total phosphorous (TP), 0.006 mg L^{-1} of soluble reactive phosphorous (SRP), and 0.37 mg L^- of TN. Two weeks later, the mesocosms were inoculated with zooplankton. For this purpose, 10 vertical and 10 horizontal hauls (approximate horizontal haul was 100 m each) were performed with zooplankton nets on two nearby lakes, Eymir and Mogan. The hauls were mixed with 20 L of water, and 750 mL of the zooplankton sample from each lake was added to each mesocosm. The next day, aquatic macroinvertebrates of various taxonomic groups (Chironomidae, Trichoptera, Ephemeroptera, Gammaridae, Odonata, Hirudinea, and Lymnea) were added in equal proportions. The invertebrates were collected from Lakes Mogan and Eymir with a benthic grab, as well as with kick-nets on a nearby stream that feeds Lake Mogan. Three flat pebbles with an approximate sediment contact surface area of 20–25 cm^2 were added to each tank to provide

additional cover for invertebrates. A week later, 7 shoots of *Potamogeton pectinatus* and 7 shoots of *Potamogeton perfoliatus* (approximate length of 5–10 cm) macrophytes were planted into each mesocosm. Immediately following, 8 topmouth gudgeons (*Pseudorasbora parva*) were added to each mesocosm. Great care was taken to ensure the same biomass of fish (equal distribution of size) in each tank, which was 9–10 g m^{-3}.

The sampling procedure began May 4th, 2014 (Day 0), one day after fish addition. The experiment lasted for 78 days, concluding July 20, 2014. A control group of 3 random mesocosms was selected, while the other 6, in two clusters of 3 random tanks, were experimental groups. Sample size of mesocosms (N=3 per group) was selected based on OECD recommendation as a standard operating procedure for mesocosms studies (OECD, 2006). In the experimental groups, E171 commercial food grade TiO_2 was added 5 times a week (Monday to Friday at 11:00 AM) at a concentration of either 25 µg L^{-1} or 250 µg L^{-1} per treatment, which was triplicated. For this purpose, a stock suspension of 25 g L^{-1} was prepared with deionized water. A commercial sample of human food grade E171 TiO_2 C.I. 77891 manufactured by Fiorio Colori Spa of Italy was obtained through Pharmorgana GmbH in Eppstein, Germany. According to the manufacturer, the product was of 99% purity. Control mesocosms received 10 mL of deionized water 5 times a week. Water depth was checked weekly, and the TiO_2 suspension was adjusted accordingly to water volume to maintain a constant addition of 25 µg L^{-1} or 250 µg L^{-1}. These two concentrations were selected based on the literature. A concentration of 25 µg L^{-1} is the daily dose that aquatic ecosystems may receive from wastewater treatment plants after filtration (Westerhoff et al., 2011) and is close to the highest predicted concentration in surface water based on a high emission scenario (Mueller and Nowack, 2008). A concentration of 250 µg L^{-1} was selected as a worst case scenario by applying a 10X factor. This concentration could potentially enter aquatic environments through urban runoff or in cases where wastewater treatment facilities are not working or not present (Kaegi et al., 2008; Kiser et al., 2009; Westerhoff et al., 2011). We assumed a very high sedimentation rate of TiO_2 based on published data of nanoparticle sedimentation in

conditions that simulate shallow lakes (Keller et al., 2010; Velzeboer et al., 2014); thus, the addition of TiO_2 was performed five times per week in order to simulate nanoparticle "snowing" effect which would normally occur in the environment. At days 0, 30, and 60, 0.0105 mg L^{-1} of TP and 0.18 mg L^{-1} of TN were added to each mesocosm in the form of $Na_2HPO_4*2(H_2O)$ or $Ca(NO_3)_2$ $*4(H_2O)$, respectively. These values are 30% of the nutrient concentration from day minus 10. Nutrients were added to maintain primary production and avoid nutrient limitation through biological or sediment retention. In a previous similar mesocosm setup, monthly nutrient retention was 20–50% of the available pool (Landkildehus et al., 2014).

Nanoparticle characterization

A Brunauer-Emmett-Teller (BET) surface area analysis of E171 TiO_2 powder was performed with Autosorb iQ Station 1 in an N_2 atmosphere. Thermo Scientific K-Alpha was used to carry out X-ray photoelectron spectroscopy (XPS) analyses. The Mg Kα (1253.6 eV) X-ray source was operated at 300 W. A pass energy of 117.40 eV was used for the survey spectra. The spectra were recorded using a 60° take-off angle relative to the normal surface. X-ray diffraction measurements were made using a Pananalytical X'pert Pro multipurpose X-ray diffractometer in reflection geometry. CuKα radiation (λ = 0.154 nm) was used by operating at 40 kV and 40 mA. Measurements were made in the 2θ range from 1° to 80° in steps of 0.05°. Transmission electron microscopic (TEM) images were obtained for E171 using an FEI Tecnai G2 F30. Samples were prepared by drop casting 1 to 2 drops of particle dispersions in ethanol onto a carbon-coated copper grid. Atomic Force Microscopy (AFM) was performed with PSIA XE-100E force spectroscopy with microfabricated Silicon cantilevers (Olympus OMCL-AC160TS-W2) having a spring constant of 40 N/mm in tapping mode. The hydrodynamic radius and the zeta potential of the TiO_2 nanoparticles were measured with Malvern ZetaNano ZS at 25 °C. TiO_2 suspensions were prepared with 25 μg L^{-1} and 250 μg L^{-1} concentrations in two different media (deionized water and lake water). These suspensions were not sonicated and were prepared in a same manner as daily made suspensions for mesocosms exposure. Average hydrodynamic radius was

measured every 5 minutes for first 60 minutes after preparation. An additional measurement after 24 h was executed as well. Such measurements were performed in order to look at suspension instability over the course of time as high sedimentation was expected. Zeta potentials were measured after 15 min of suspension preparation. An U-shaped capillary cell DTS1060 was used to estimate both the zeta potential and the hydrodynamic radius using a He-Ne laser source of 5 mW at 633 nm wavelength.

Sedimentation and effective exposure concentrations were measured by inductively coupled plasma mass spectrometry (ICP-MS). For this purpose, one meter long glass sedimentation tube with 5 cm diameter was used. Sedimentation tubes (N =3) were filled with lake water and spiked with 250 μg L^{-1} of TiO_2. With a long syringe water samples were taken at 1, 4, 8, and 24 h after spiking. Each time water was collected from 10, 50, and 90 cm of the column depth. In addition, a control sample consisting only of lake water was included in order to determine background concentration of titanium ions in the lake water. Water samples were prepared for ICP-MS analysis according to the standard methodology - Method EPA6020A ICP-MS. Concentrations of titanium isotopes 47 and 49 were measured by Perkin Elmer NexION 300x, corrected for natural abundance, averaged, and later converted to TiO_2 concentration using the following formula:

TiO_2 conc. = (Ti conc. of the experimental sample - background Ti conc. of the lake water) X mass ratio of TiO_2/Ti.

Sampling procedure

During the first three weeks, samplings and measurements were performed weekly, starting with day 0. After that, a bi-weekly schedule was followed. All samples were collected and all measurements were performed at the same time of day, before the daily TiO_2 addition. Each time, water temperature, conductivity, total dissolved solids, salinity, percentage of oxygen saturation, total dissolved oxygen, and pH were measured in each mesocosm at a depth of 10 cm, 50 cm, and just above the bottom. Measurements were performed with a YSI 556 MPS multiprobe field meter (YSI

Incorporated, OH, USA). Water transparency was measured with a Secchi disk, while depth was measured with a Laylin SM5 depthmeter portable sounder (Laylin Associates, Unionville, USA).

During each sampling, photosyntethically active radiation (PAR light) was measured in each mesocosm with a Li-250A light meter (Li-Cor, NE, USA), starting just above the water surface and continuing until 70 cm water depth in intervals of 10 cm. All data were expressed as a percentage of surface PAR intensity for the given mesocosm to compensate for different weather conditions. PAR light was only measured until day 51, after which it became impossible due to macrophyte growth.

At each sampling, 20 L was collected from the middle of the water column of each mesocosm with an improvised PVC pipe device (5 cm diameter) with a valve on one end and then mixed in a bucket. Of those 20 L, one liter total was taken for nutrient, suspended solids, and Chl-a analyses, while 6 L were filtered through a 20 µm mesh filter to collect zooplankton. Both the filtered water and remaining unfiltered water were returned to the corresponding mesocosm after sampling. Zooplankton was preserved in 4% Lugol's solution. Chl-a pigment and carotenoid content were determined in phytoplankton by ethanol extraction in triplicate (Jespersen and Christoffersen, 1987). Measurements were performed with a Lambda 35 UV/VIS spectrophotometer (PerkinElmer Inc., MA, USA). In addition to Chl-a and carotenoids, 480/663 and 430/410 ratios were calculated, and phytoplankton was grouped into four categories: a) healthy phytoplankton (480/663 < 1.3 and 430/410 > 1.2), b) heavily grazed phytoplankton containing degradation products (480/663 < 1.3 and 430/410 < 1.2), c) nitrogen deficient phytoplankton (480/663 > 1.3 and 430/410 > 1.2), and d) heavily contaminated phytoplankton containing excessive suspended solids (480/663 > 1.3 and 430/410 < 1.2). Phytoplankton wet biomass was estimated from the concentration of Chl-a, assuming one unit of phytoplankton wet weight equaled 0.505% of Chl-a (Kasprzak et al., 2008), and converted to dry biomass with a factor of 0.2 (Parparov et al., 2014). The ratio of zooplankton to phytoplankton dry biomass was calculated as an indicator of zooplankton grazing pressure on phytoplankton.

A periphyton growth experiment was also undertaken in all mesocosms. Transparent polypropylene strips (21 mm × 297 mm each) with a slightly textured surface (IBICO®, Germany) were placed 30 cm from the mesocosm wall, 50 cm below the water surface. Three strips were introduced to each mesocosm for 30 days to allow periphyton colonization, and then replaced with a new set. Both wet and dry biomass were calculated after scraping the periphyton from the strips.

Total suspended solids were quantified at each sampling by filtering a known amount of water from each mesocosm and quantifying the dry mass of residue on the filter.

NH_4^+-N, NO_2+NO_3, and TN were measured after each sampling using the Skalar Autoanalyzer (San++ Automated Wet Chemistry Analyzer, Skalar Analytical, B.V., Breda, The Netherlands) according to manufacturer protocol. To determine TP, the acid hydrolysis method was used (Mackereth et al., 1978). To determine SRP, filtered water was processed using the molybdate reaction method (Mackereth et al., 1978).

Zooplankton specimens were counted under the microscope (LEICA MZ 16 stereomicroscope). Length measurements were taken, and the zooplankton dry biomass was calculated for each taxon independently according to previously published formulae for *Alona sp.* (Rosen, 1981), *Bosmina sp.* (Michaloudi, 2005), *Daphnia sp.* (Bottrell et al., 1976; McCauley, 1984), and copepods (Bottrell et al., 1976). The mass of each nauplii was considered to be 0.25 µg (Culver et al., 1985). The volume of rotifers was calculated from their length for each taxon independently (Ruttner-Kolisko, 1977), and for unidentified rotifers (< 1 % of all rotifers by count), the formula $V = 0.124\ a^3$ was used to calculate volume as an average of all rotifer taxa where *a* was the length. Rotifer volume was later transformed to wet weight, assuming a specific gravity of rotifer body size equal to 1 (1 µg = 10^6 μm^3(Bottrell et al., 1976). The dry weight of rotifers is estimated to be 4% of the wet weight for *Asplanchna spp.* and 10% for all others (Bottrell et al., 1976).

Starting at day 36, when the growth of the macrophytes became visible, the percent plant volume inhabited (PVI%) was calculated using plant surface coverage, height, and water depth.

At the end of the experiment, all macrophytes were harvested with a hand rake and taken to the laboratory, where they were cleaned and dried at 105° C for 24 hours to determine dry mass. Surface sediment samples (0-5 cm) were also retrieved with a KC-Denmark Kajak Corer (5.2 cm internal diameter) to collect chironomids. Six cores were taken from each mesocosm. Chironomid larvae were preserved in ethanol and their abundance and biomass were determined.

Statistics

Initial values of all parameters prior to the start of the experiment (day 0 samples) and values for parameters sampled only at the end of the experiment (day 78 sample of macrophytes, fish, and chironomids) were analyzed with a one way ANOVA. For significant differences, a post hoc comparison of means between a single control and two experimental groups was performed using Dunnett's test. All other data were tested for treatment, time, and treatment x time interaction using split-plot repeated measures ANOVA (split-plot rANOVA), followed by Dunnett's test if significant difference was detected. Data were logtransformed before analysis where appropriate to reduce skewness and to approximate to normal distribution. P-value equal to or less than 0.05 was considered statistically significant, unless otherwise noted. Post-hoc observed power analysis was also performed (Supporting Table ST1). Statistica 12.0 software (StatSoft) was used for all analyses. In some cases, for better visual representation of data, figures are presented both in the $\mu g\ L^{-1}$ and percentage of control units.

Results

TiO_2 characterization

According to BET analysis, the specific surface area of the TiO_2 was calculated to be 6.137 m^2 g^{-1}, while pore volume was 0.123 cc g^{-1} and pore diameter was 2.968 nm.

All detected diffraction peaks in XRD analysis were well defined and can be perfectly assigned to the anatase crystal structure. The sharp peaks corresponded to the (101), (004), (200), (105), (211), (204), (116), (220), and (215) crystal planes of TiO_2 particles. No characteristic peaks referring to other crystalline forms were detected (Figure 1A).

The XPS survey scan of the E171 sample is shown in Figure 1B-D. The Ti2p spectra exhibit a Ti2p3/2 peak at 463.8 eV and a 2p1/2 peak at 458.0 eV, characteristic of TiO_2 (Figure 1C). The O1s spectra show a main peak at 529.2 eV, assigned to oxygen that is bound to tetravalent Ti ions, and a shoulder at ~532.5 eV, which implies that the surface is partially covered with hydroxide OH groups (Figure 1D). The titanium:oxygen ratio also indicates that the TiO_2 is of anatase crystal structure.

The TEM investigation revealed that E171 TiO_2 has broad size distributions with sharp, clean, and well-defined edges. Particle size varies between 50 and 300 nm (Figure 1E), and the particles form aggregates in the ethanol suspension. AFM analysis revealed more precisely the diameter of E171 TiO_2 particles. According to the AFM mean, particle size ± standard error of the mean (SEM) was 167 ± 50 nm.

According to DLS measurement in pure water, the particle diameter is below 100 nm for approximately 30 % of TiO_2 particles. The results in Table 1 shows the average hydrodynamic diameters of TiO_2 nanoparticles in two different media and at two different concentrations over the course of time. TiO_2 suspension in lake water was making larger aggregates than in deionized water and the aggregate size in the lake water was reduced when the nanoparticle concentration increased from 25 to 250 μg L^{-1}. The suspension was highly polydispersed with a PDI of 0.9-1. The ζ-potential values measured for the dispersions of the TiO_2 NPs in deionized water and lake water were slightly

different. ζ-potential ranged from -12.2 ± 0.4 to -20.2 ± 0.4 mV (mean ± SD) for TiO_2 in deionized water and -6.8 ± 0.3 to -7.4 ± 0.3 mV for TiO_2 in lake water, respectively. Both dispersions are unstable because the ζ-potential value is higher than -30 mV and lower than +30 mV, which are considered the lowest and the upper limits for a stable colloidal dispersion. The average hydrodynamic diameter of the aggregates (Table 1) was high, and it was evident that the aggregates were settling down fast to the bottom of the testing chamber within first hour. Such rapid sedimentation resulted in a decline of the average hydrodynamic diameter of the remaining aggregates present in the suspension.

Sedimentation of 250 μg L^{-1} TiO_2 particles in the lake water occurred, as expected. As determined by ICP-MS at least 48.5 % of the initial 250 μg L^{-1} TiO_2 concentration added to the test system was lost from the suspension after 24 h; most likely by settling to the bottom (Supporting Figure S2). This loss of concentration was most likely achieved through fast sedimentation of the largest aggregates (responsible for the considerable share of mass %) as evident by a decline of suspension average hydrodynamic diameter in the first hour determined by DLS (Table 1). There was a statistically significant difference in sedimentation related to time span (rANOVA $P < 0.05$). As the time elapsed the sedimentation become more rapid and the average TiO_2 concentration ± SEM was: 238.3 ± 13.8; 230.7 ± 18.0; 182.5 ± 9.5; and 128.8 ± 12.5 μg L^{-1} after 1, 4, 8, and 24 h, respectively. The biggest decrease in concentration per hour due to sedimentation occurred between the hours 4-8 (12.05 μg L^{-1} h^{-1}), as opposed to the first hour (11.70 μg L^{-1} h^{-1}); the hours 1-4 (2.53 μg L^{-1} h^{-1}); or the hours 8-24 (3.58 μg L^{-1} h^{-1}). No depth related stratification of TiO_2 suspension occurred in the system (rANOVA $P > 0.05$), although, on average over all time points, concentration of TiO_2 increased with the water column depth and was: 178.6 ± 17.2; 187.7 ± 16.6; and 229.5 ± 17.1 (mean ± SEM) μg L^{-1} for 10, 50, and 90 cm water column depth, respectively.

Physicochemical effects

No statistical differences were found in any of the measured parameters between any tanks on day 0 before the start of the experiment. Thus all groups had similar conditions. During the experiment, based on the split-plot rANOVA output, no significant difference was found between the treatments for dissolved oxygen, water temperature, salinity, conductivity, water transparency, pH, total dissolved solids, and total suspended solids at any of the measured water column depths (Table 2). The total water volume per mesocosm was reduced by about 30% toward the end of experiment due to evaporation, in accordance with established norms (OECD, 2006). PAR light intensity (Figure 2) increased 5% on average throughout the water column in the TiO_2 250 µg L^{-1} treatment compared to the control (Dunnett's test $P < 0.01$). There was no significant difference between the TiO_2 25 µg L^{-1} treatment and the control.

TN, NH_4^+-N, NO_2+NO_3, and TP levels were also unaffected by the treatments (Table 2). However, there was a significant and dose-dependent reduction of SRP levels in TiO_2 treatments compared to the control (Figure 3A-C). Overall, the concentration was reduced by 15% and 23% in the TiO_2 25 µg L^{-1} and TiO_2 250 µg L^{-1} treatments, respectively, compared to the control (Figure 3C).

Biological effects

The treatment of mesocosms with TiO_2 did not induce change in the concentration of Chl-a, carotenoids, or 480/663 and 430/410 ratios (rANOVA $P >> 0.1$) when compared to the control (Figure 4A-C).

Analysis of the zooplankton biomass revealed that TiO_2 did not induce any change in the biomass of Cladocera or Copepoda, separately or combined (Figure 5A). However, the biomass of Rotifera was significantly reduced in the TiO_2 25 µg L^{-1} (by 32%) and TiO_2 250 µg L^{-1} (57%) treatments (Dunnett's test $P < 0.01$) when compared to the control (Figure 5B-C). The ratio of zooplankton to phytoplankton dry biomass was not significantly different when TiO_2 treatments were compared with the control; thus, there was no difference in zooplankton grazing pressure on phytoplankton.

There was no statistical difference in macrophytes PVI% between the treatments and control at any single point in time. At the very end of the experiment, the average PVI% was 86. Also, no difference was found between the treatments and control in the biomass of *P. pectinatus* or *P. perfoliatus* at the end of the experiment. After the macrophytes were harvested, washed, and separated, two additional species were detected in each mesocosm: *Chara sp.* and *Najas sp*. These species were not initially planted but grew from seeds in the sediment. There was no difference in the biomass of either *Chara sp.* or *Najas sp.* between the treatments and control. Also, there was no difference in the total biomass of all of the macrophytes or periphyton biomass between the treatments and control.

Analysis of abundance and biomass of *Chironomus plumosus* did not reveal any statistical difference among treatments (Table 2).

During the experiment, 2 out of 72 fish died. One died in the TiO_2 250 µg L^{-1} group; the second died in the control group. There were no visible signs of lesions or infection on any deceased or living fish. The majority of the fish were recovered with a net after the experiment, and neither the average mass per fish nor the estimated biomass were statistically different between the treatments and control (Table 2).

Discussion and conclusion

E171 from Fiorio Colori Spa has been previously characterized as having (a) an average particle size of 117 nm, with at least 20% of the particles by number having a diameter < 100 nm; (b) anatase crystal structure; (c) 0.13% of Al_2O_3 impurities and < 1% of SiO_2 by dry weight; and (d) an isoelectric point < 2.5 ((Yang et al., 2014). The same producer's sample has been partially characterized elsewhere as having an average particle size of 110 nm, with at least 36% of the particles by number having a diameter < 100 nm (Weir et al., 2012). Although the results of the present study are not exactly the same as those of previous studies, they are fairly similar. The present study found the average primary particle size of the sample to be 167 nm, with pure anatase crystal structure partially covered with

hydroxide OH groups. Previously, it was determined that E171 characteristics can vary significantly among producers (Yang et al., 2014); however, the present study indicates that even different batches from the same producer may differ. However, methodology and measuring instruments may also contribute to observed discrepancies.

The ability of E171 TiO_2 to reduce SRP concentrations was significant in the present study. It is known that nano-TiO_2 has a high adsorption rate of phosphorous (28.3 mg g^{-1}) and a very low desorption capacity; thus, obtained results are not unexpected (Moharami and Jalali, 2014). However, because a total of 1.42 mg L^{-1} or 14.25 mg L^{-1} of E171 TiO_2 was added to two experimental mesocosm groups over 78 days of exposure and the observed decrease in SRP concentration was 1 and 2 µg L^{-1}, respectively, when compared to the control, the TiO_2 efficiently removed a maximum of 0.7 mg of SRP per g of TiO_2. This is 30X less than the previously determined adsorption coefficient. The previous study (Moharami and Jalali, 2014) was performed under optimum conditions for adsorption time, temperature, pH, and adsorbent dosage, while the present results were obtained under natural conditions. Although the TiO_2 reduced SRP concentration in the mesocosms, this change had no biological consequences since the biomass production capacity of the phytoplankton and macrophytes was not limited by the phosphorous.

TiO_2 nanoparticles are photoactive and are significantly more toxic under natural sunlight to a variety of aquatic species (Jovanović, 2015b). Aggregation of TiO_2 nanoparticles and biological surface coating both of phytoplankton (Miller et al., 2012) and zooplankton (Dabrunz et al., 2011) has been described as the reason for this toxicity expression (Jovanović, 2015b). TiO_2 phototoxicity is manifested by the particle production of reactive oxygen species, which cause oxidative damage (Li et al., 2014; Miller et al., 2012). Additionally, the inhibition of molting, reproduction, swimming, growth, or available food reduction for zooplankton (Campos et al., 2013; Dabrunz et al., 2011; Jacobasch et al., 2014) is yet another mode of action. All of these toxic effects would essentially reduce the available biomass of the target taxon in an ecosystem. However, such toxic effects have been demonstrated only

in laboratory settings using standardized water media with a single species environment and may be lost in a multispecies ecosystem environment. Nekton organisms may actively seek shelter from sunlight, minimizing the phototoxicity effects of TiO_2. Food partitioning of consumer organisms in the presence of TiO_2 to avoid increased competition may be another mechanism to maintain ecosystem balance.

In an aquatic ecosystem, TiO_2 particles can settle at the bottom rapidly due to presence of natural organic matter or can even be covered by sediment. In fact, it was previously suggested that nano-TiO_2 has a significant sedimentation rate (Keller et al., 2010; Velzeboer et al., 2014). The present study also demonstrated that concentration of suspended nano-TiO_2 in lake water decreased approximately 50% within the 24 h period due to sedimentation. Concomitantly, rapid aggregation of the particles was detected. Such behavior of nanoparticles introduces a new variable - the "nanoparticle snowing effect". The snowing effect normally occurs in the aquatic environment within the proximity of nanoparticle pollution sources due to the persistent input. While it is difficult to simulate such effect in the conventional laboratory toxicity tests without multispecies environment, the present outdoor mesocosm study provides conditions close to reality. This is especially important since concentration of nano-TiO_2 is not unequivocal in the aquatic ecosystem due to the sedimentation and aggregation; and it is changing dynamically on a spatiotemporal scale. As a result, different species/individuals, even different parts of a single individual, (e.g., macrophytes) will be exposed to a different concentration of nano-TiO_2 based on their biological traits and ecological roles. Individuals from two different ecosystem compartments may be exposed to equal effective exposure concentrations expressed as g L^{-1}. At the same time, they may also be exposed to two drastically unequal concentrations if expressed as g m^{-2} or particle# L^{-1}. Although the outdoor mesocosm studies are more realistic compared to laboratory toxicity tests in terms of risk assessment, quantification and characterization of nanoparticles are much more difficult. Real time quantification and characterization of nanoparticles in a mesocosm

on a spatiotemporal scale are currently impossible due to technical restrictions, while available snapshot analyses provide only limited data regarding effective exposure concentration.

The present study could not demonstrate any effects of environmentally relevant concentrations of E171 TiO_2 on biomass changes of phytoplankton, Cladocera, Copepoda, macrophytes, *C. plumosus*, or *P. parva* in mesocosms over a prolonged period of exposure. The only apparent effect was for Rotifera, which experienced a significant reduction in biomass compared to the control. Very little literature exists on the effect of nanoparticles or TiO_2 on rotifers. Previously, it was demonstrated that rotifers are able to ingest plastic nanoparticles of various sizes (Snell and Hicks, 2011). Nano-TiO_2 toxicity has been investigated in only one euryhaline rotifer species, *Brachionus plicatilis*, and it caused growth inhibition at a concentration far exceeding those of the present study (Clément et al., 2013). The five most common rotifer taxa observed in the present study were Hexarthra, Polyarthra, Keratella, Asplanchna, and Lecane, accounting for more than 90% of all counted individuals. Thus, there is not enough scientific information to explain observed effects. A possible reason for the rotifer biomass reduction may be biological surface coating with nano-TiO_2, which was previously described for other zooplankton organisms (Dabrunz et al., 2011) and led to impaired food filtering or reproduction. In addition, rotifers are inefficient swimmers, spending up to 60% of their metabolism energy for locomotion (Epp and Lewis, 1984). Thus, coating with a material of high specific gravity such as TiO_2 (3.77–4.23 g cm^{-3}) may induce starvation and exhaustion or may cause rotifers to sink. Reduced swimming capability likely increases the risk of falling prey to copepods or other zooplankton species. Although rotifers play an important role in many freshwater plankton communities, they are not considered a keystone species (Waltz, 1997). They may, however, play a significant role in the microbial web (Arndt, 1993).

In conclusion, environmentally relevant concentrations of E171 TiO_2 nanoparticles may negatively affect certain parameters and taxa of the freshwater lentic aquatic ecosystem. In particular, treatments of 25 µg L^{-1} TiO_2 and 250 µg L^{-1} TiO_2 caused a reduction in the amount of available soluble

reactive phosphorus in experimental mesocosms by 15% and 23%, respectively. The biomass of Rotifera was significantly reduced by 32% and 57% in the TiO_2 25 µg L^{-1} and TiO_2 250 µg L^{-1} treatments, respectively, when compared to the control. Finally, the intensity of PAR light increased by 5% throughout the water column in the TiO_2 250 µg L^{-1} treatment. However, none of these negative effects were significant enough to affect the overall function of the ecosystem, as there were no cascade effects leading to a major change in its trophic state or primary production.

Acknowledgements

The present research was partially supported by B. Jovanović's Marie Curie FP7 Career Integration Grant within the 7th European Union Framework Programme, Project No. PCIG13-GA-2013-618006. B. Jovanović also extends acknowledgement to the Scientific and Technological Research Council of Turkey (TUBITAK) for partial support through the visiting scientist fellowship programme, TUBITAK 2221. M. Beklioğlu was supported by the MARS project (Managing Aquatic ecosystems and water Resources under multiple Stress), funded under the 7th EU Framework Programme, Theme 6 (Environment including Climate Change), Contract No. 603378 (http://www.mars-project.eu).We would also like to extend our gratitude to the TUBITAK Marmara Research Center of Turkey, Gebze - Kocaeli, for the help with ICP-MS analysis.

References

Altomare, M., Selli, E., 2013. Effects of metal nanoparticles deposition on the photocatalytic oxidation of ammonia in TiO_2 aqueous suspensions. Catalysis Today 209, 127-133.

Arndt, H., 1993. Rotifers as predators on components of the microbial web (bacteria, heterotrophic flagellates, ciliates) — a review. Hydrobiologia 255-256, 231-246.

Bottrell, H.H., Duncan, A., Gliwicz, Z.M., Grygierek, E., Herzig, A., Hillbricht-Ilkowska, A., Kurasawa, H., Larsson, P., Weglenska, T., 1976. A review of some problems in zooplankton production studies. Norw. J. Zool. 24, 419-456.

Campos, B., Rivetti, C., Rosenkranz, P., Navas, J.M., Barata, C., 2013. Effects of nanoparticles of TiO_2 on food depletion and life-history responses of *Daphnia magna*. Aquatic Toxicology 130–131, 174-183.

Cheng, T.C., Chang, C.Y., Chang, C.I., Hwang, C.J., Hsu, H.C., Wang, D.Y., Yao, K.S., 2008. Photocatalytic bactericidal effect of TiO_2 film on fish pathogens. Surface and Coatings Technology 203, 925-927.

Clément, L., Hurel, C., Marmier, N., 2013. Toxicity of TiO_2 nanoparticles to cladocerans, algae, rotifers and plants – Effects of size and crystalline structure. Chemosphere 90, 1083-1090.

Coleman, H.M., Marquis, C.P., Scott, J.A., Chin, S.S., Amal, R., 2005. Bactericidal effects of titanium dioxide-based photocatalysts. Chemical Engineering Journal 113, 55-63.

Culver, D.A., Boucherle, M.M., Bean, D.J., Fletcher, J.W., 1985. Biomass of freshwater crustacean zooplankton from length–weight regressions. Canadian Journal of Fisheries and Aquatic Sciences 42, 1380-1390.

Dabrunz, A., Duester, L., Prasse, C., Seitz, F., Rosenfeldt, R., Schilde, C., Schaumann, G.E., Schulz, R., 2011. Biological surface coating and molting inhibition as mechanisms of TiO_2 nanoparticle toxicity in *Daphnia magna*. PLoS ONE 6, e20112.

Epp, R.W., Lewis, W.M., 1984. Cost and speed of locomotion for rotifers. Oecologia 61, 289-292.

European Commission, 2008. Follow-up to the 6th Meeting of the REACH Competent Authorities for the implementation of Regulation (EC) 1907/2006; (REACH). http://ec.europa.eu/environment/chemicals/reach/pdf/nanomaterials.pdf

European Parliament, 2006. Regulation (EC) No. 1907/2006 of the European Parliament and of the Council of 18 December 2006 concerning the Registration, Evaluation, Authorisation and Restriction of Chemicals (REACH) (OJ L 396, 30.12.2006).

Haghighi, M., Heidarian, S., Teixeira da Silva, J., 2012. The effect of titanium amendment in N-withholding nutrient solution on physiological and photosynthesis attributes and micronutrient uptake of tomato. Biol Trace Elem Res 150, 381-390.

Huang, Z., Maness, P.-C., Blake, D.M., Wolfrum, E.J., Smolinski, S.L., Jacoby, W.A., 2000. Bactericidal mode of titanium dioxide photocatalysis. Journal of Photochemistry and Photobiology A: Chemistry 130, 163-170.

Jacobasch, C., Völker, C., Giebner, S., Völker, J., Alsenz, H., Potouridis, T., Heidenreich, H., Kayser, G., Oehlmann, J., Oetken, M., 2014. Long-term effects of nanoscaled titanium dioxide on the cladoceran *Daphnia magna* over six generations. Environmental Pollution 186, 180-186.

Jespersen, A.M., Christoffersen, K., 1987. Measurements of chlorophyll a from phytoplankton using ethanol as extraction solvent. Archiv fu¨r Hydrobiologie 109, 445-454.

Jovanović, B., 2015a. Critical review of public health regulations of titanium dioxide, a human food additive. Integrated Environmental Assessment and Management 11, 10-20.

Jovanović, B., 2015b. Review of titanium dioxide nanoparticle phototoxicity: Developing a phototoxicity ratio to correct the endpoint values of toxicity tests. Environmental Toxicology and Chemistry 34, 1070-1077.

Kaegi, R., Ulrich, A., Sinnet, B., Vonbank, R., Wichser, A., Zuleeg, S., Simmler, H., Brunner, S., Vonmont, H., Burkhardt, M., Boller, M., 2008. Synthetic TiO_2 nanoparticle emission from exterior facades into the aquatic environment. Environmental Pollution 156, 233-239.

Kasprzak, P., Padisák, J., Koschel, R., Krienitz, L., Gervais, F., 2008. Chlorophyll a concentration across a trophic gradient of lakes: An estimator of phytoplankton biomass? Limnologica - Ecology and Management of Inland Waters 38, 327-338.

Keller, A.A., Wang, H., Zhou, D., Lenihan, H.S., Cherr, G., Cardinale, B.J., Miller, R., Ji, Z., 2010. Stability and aggregation of metal oxide nanoparticles in natural aqueous matrices. Environmental Science & Technology 44, 1962-1967.

Kim, E., Kim, S.-H., Kim, H.-C., Lee, S., Lee, S., Jeong, S., 2011. Growth inhibition of aquatic plant caused by silver and titanium oxide nanoparticles. Toxicol. Environ. Health Sci. 3, 1-6.

Kiser, M.A., Westerhoff, P., Benn, T., Wang, Y., Pérez-Rivera, J., Hristovski, K., 2009. Titanium nanomaterial removal and release from wastewater treatment plants. Environmental Science & Technology 43, 6757-6763.

Kulacki, K.J., Cardinale, B.J., 2012. Effects of nano-titanium dioxide on freshwater algal population dynamics. PLoS ONE 7, e47130.

Kulacki, K.J., Cardinale, B.J., Keller, A.A., Bier, R., Dickson, H., 2012. How do stream organisms respond to, and influence, the concentration of titanium dioxide nanoparticles? A mesocosm study with algae and herbivores. Environmental Toxicology and Chemistry 31, 2414-2422.

Landkildehus, F., Søndergaard, M., Beklioglu, M., Adrian, R., Angeler, D.G., Hejzlar, J., Papastergiadou, E., Zingel, P., Çakiroğlu, A.I., Scharfenberger, U., Drakare, S., Nõges, T., Sorf, M., Stefanidis, K., Tavşanoğlu, Ü.N., Trigal, C., Mahdy, A., Papadaki, C., Tuvikene, L., Larsen, S.E., Kernan, M., Jeppesen, E., 2014. Climate change effects on shallow lakes: design and preliminary results of a cross-European climate gradient mesocosm experiment Estonian Journal of Ecology 63, 71-89.

Lehtinen, K.-J., Larsson, Å., Klingstedt, G., 1984. Physiological disturbances in rainbow trout, Salmo gairdneri (R.), exposed at two temperatures to effluents from a titanium dioxide industry. Aquatic Toxicology 5, 155-166.

Li, S., Pan, X., Wallis, L.K., Fan, Z., Chen, Z., Diamond, S.A., 2014. Comparison of TiO_2 nanoparticle and graphene–TiO_2 nanoparticle composite phototoxicity to *Daphnia magna* and *Oryzias latipes*. Chemosphere 112, 62-69.

Liu, X., Chen, G., Erwin, J.G., Adam, N.K., Su, C., 2013. Release of phosphorous impurity from TiO_2 anatase and rutile nanoparticles in aquatic environments and its implications. Water Research 47, 6149-6156.

Luo, Z., Wang, Z., Wei, Q., Yan, C., Liu, F., 2011. Effects of engineered nano-titanium dioxide on pore surface properties and phosphorus adsorption of sediment: Its environmental implications. Journal of Hazardous Materials 192, 1364-1369.

Mackereth, F.G.H., Heron, J., alling, J.F., 1978. Water analysis: Some revised methods for limnologists. Freshwater Biological Association, Ambleside, 36.

McCauley, E., 1984. The estimation of the abundance and biomass of zooplankton in samples. In Downing, J. A. & F. H. Rigler (Eds.): A manual on methods for the assessment of secondary productivity in freshwaters, 228-265.

Michaloudi, E., 2005. Dry weights of the zooplankton of Lake Mikri Prespa (Macedonia, Greece). Belg. J. Zool. 135, 223-227.

Miller, R.J., Bennett, S., Keller, A.A., Pease, S., Lenihan, H.S., 2012. TiO_2 nanoparticles are phototoxic to marine phytoplankton. PLoS ONE 7, e30321.

Moharami, S., Jalali, M., 2014. Effect of TiO_2, Al_2O_3, and Fe_3O_4 nanoparticles on phosphorus removal from aqueous solution. Environmental Progress & Sustainable Energy 33, 1209-1219.

Mueller, N.C., Nowack, B., 2008. Exposure modeling of engineered nanoparticles in the environment. Environmental Science & Technology 42, 4447-4453.
OECD, 2006. Guidance document on simulated freshwater lentic field tests (outdoor microcosms and mesocosms). OECD Environment Health and Safety Publications Series on Testing and Assessment No. 53, Paris, France. ENV/JM/MONO(2006)17.
Parparov, A., Zohary, T., Berman, T., Gal, G., 2014. Seston and organic matter. In: Lake Kinnaret; Ecology and management. Editors Zohary, T., Sukenik, A., Berman, T., and Nishri, A. Springer, New York. Aquatic Ecology Series, Vol. 6. 473-484.
Rosen, R.A., 1981. Length-dry weight relationships of some freshwater zooplankton. Journal of Freshwater Ecology 1, 225-229.
Ruttner-Kolisko, A., 1977. Suggestions for biomass calculations of plankton rotifers. Arc. Hydrobiol. Beih. Ergebn. Limnol. 8, 71-76.
Snell, T.W., Hicks, D.G., 2011. Assessing toxicity of nanoparticles using *Brachionus manjavacas* (Rotifera). Environmental Toxicology 26, 146-152.
Velzeboer, I., Quik, J.T.K., van de Meent, D., Koelmans, A.A., 2014. Rapid settling of nanoparticles due to heteroaggregation with suspended sediment. Environmental Toxicology and Chemistry 33, 1766-1773.
Waltz, N., 1997. In: Streit, B., Stadler, T., & Lively, C. M. (Eds.). Evolutionary ecology of freshwater animals: concepts and case studies. Vol. 82. Springer. pp.119-149.
Weir, A., Westerhoff, P., Fabricius, L., Hristovski, K., von Goetz, N., 2012. Titanium dioxide nanoparticles in food and personal care products. Environmental Science & Technology 46, 2242-2250.
Westerhoff, P., Song, G., Hristovski, K., Kiser, M.A., 2011. Occurrence and removal of titanium at full scale wastewater treatment plants: implications for TiO_2 nanomaterials. Journal of Environmental Monitoring 13, 1195-1203.
Windler, L., Lorenz, C., von Goetz, N., Hungerbühler, K., Amberg, M., Heuberger, M., Nowack, B., 2012. Release of titanium dioxide from textiles during washing. Environmental Science & Technology 46, 8181-8188.
Yang, Y., Doudrick, K., Bi, X., Hristovski, K., Herckes, P., Westerhoff, P., Kaegi, R., 2014. Characterization of food-grade titanium dioxide: The presence of nanosized particles. Environmental Science & Technology 48, 6391-6400.
Yeo, M.-K., Nam, D.-H., 2013. Influence of different types of nanomaterials on their bioaccumulation in a paddy microcosm: A comparison of TiO_2 nanoparticles and nanotubes. Environmental Pollution 178, 166-172.
Zheng, X., Chen, Y., Wu, R., 2011. Long-term effects of titanium dioxide nanoparticles on nitrogen and phosphorus removal from wastewater and bacterial community shift in activated sludge. Environmental Science & Technology 45, 7284-7290.

Figure captions

Figure 1
Characteristics of E171 TiO_2 particles. A: XRD patterns of the crystal structure, B: XPS spectra survey scan, C: XPS spectra of the Ti2p peak, D: XPS spectra of the O1s peak, D: TEM images of E171 TiO_2 particles.

Figure 2
Effect of TiO_2 on intensity of PAR light in the water column. Data were averaged over multiple sampling times. * indicates that the effect is statistically significant at a level of $P < 0.01$.

Figure 3
Effect of TiO_2 on SRP levels. A-B: time series; C: combined data over multiple sampling times and expressed as % of the average control from the corresponding control in time. Dashed lines represent point in time when 30% of the nutrients were added to the system based on average nutrient concentration from day minus 10. A-B - whiskers represent standard error of the mean; C - Boxes refer to standard error of the mean and whiskers to standard deviation.

Figure 4
A: time series of Chl-a concentration, B: carotenoids concentration, and C: 480/663 and 430/410 ratios across TiO_2 treatments and control group. Dashed lines represent point in time when 30% of the nutrients were added to the system based on average nutrient concentration from day minus 10. Whiskers represent standard error of the mean.

Figure 5
Effect of TiO_2 on zooplankton biomass. A: Cladocera + Copepoda time series, B: Rotifera time series, C: Rotifera combined data over multiple sampling times and expressed as % of average control from corresponding control in time. Dashed lines represent point in time when 30% of the nutrients were added to the system based on average nutrient concentration from day minus 10. A-B - whiskers represent standard error of the mean; C - Boxes refer to standard error of the mean and whiskers to standard deviation.

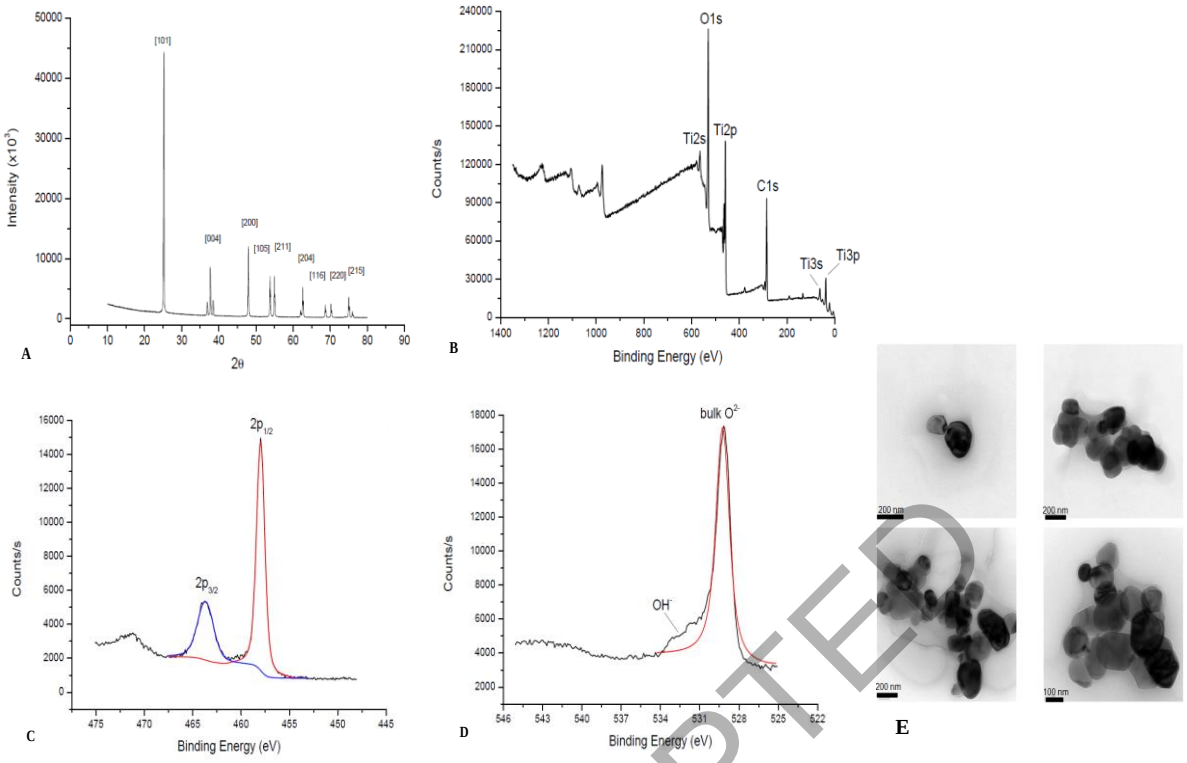

Figure 1

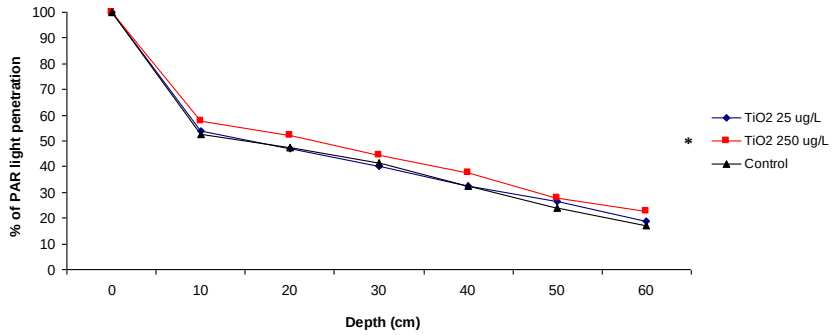

Figure 2

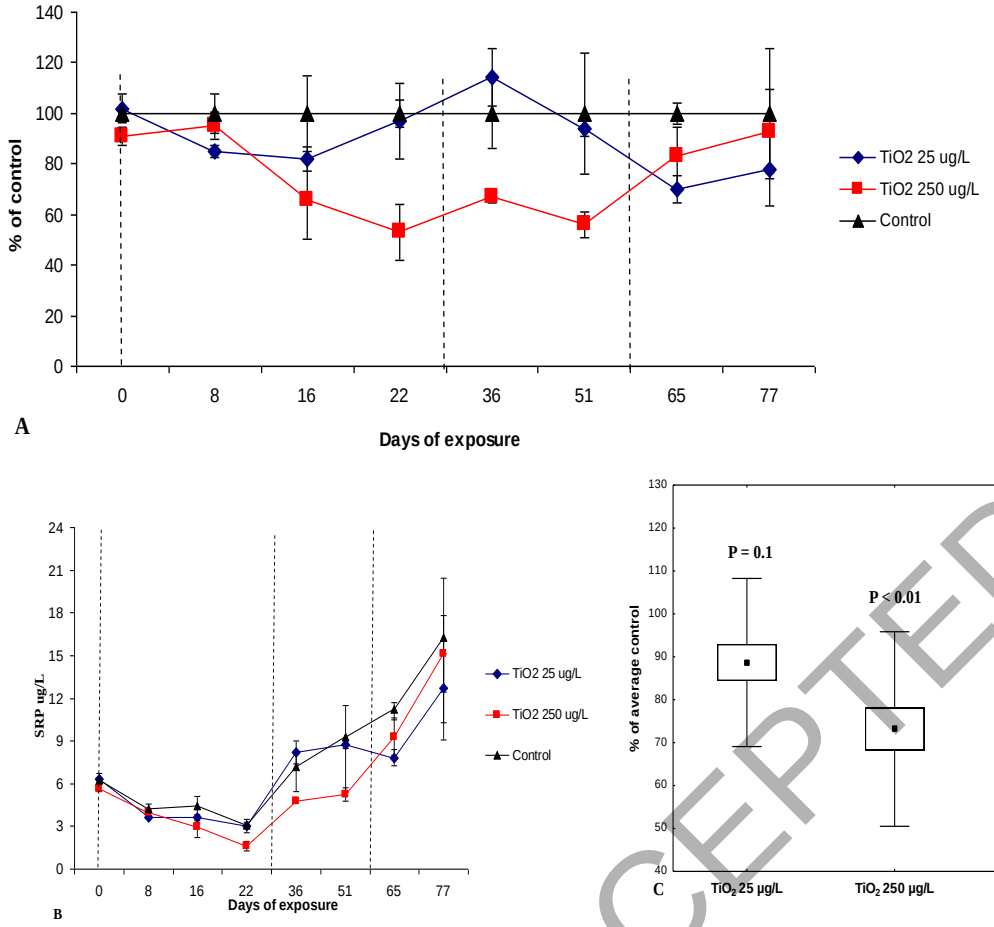

Figure 3

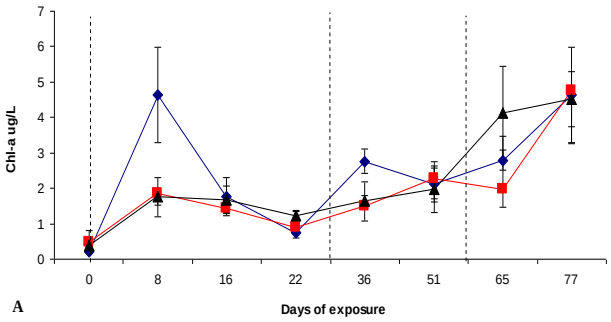

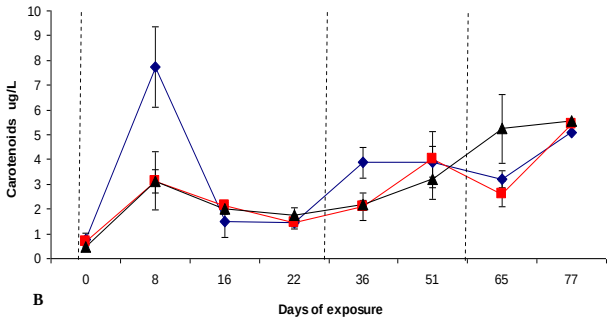

Day	480/663	430/410	480/663	430/410	480/663	430/410
	TiO2 25 ug/L		TiO2 250 ug/L		Control	
0	1.81	1.14	1.37	1.19	2.33	1.23
8	1.58	1.17	1.6	1.33	1.51	1.28
16	0.86	1.29	1.3	1.02	1.22	1.12
22	1.31	1.06	1.29	1.09	1.3	1.23
36	1.28	1.03	1.28	1.01	1.19	1.07
51	1.54	1.11	1.57	1.15	1.48	1.16
65	1.1	1.25	1.16	1.15	1.24	1.15
77	1.1	1.14	1.12	1.12	1.18	1.04

healthy phytoplankton
heavily grazed
nitrogen deficient
too much suspended solids

C

Figure 4

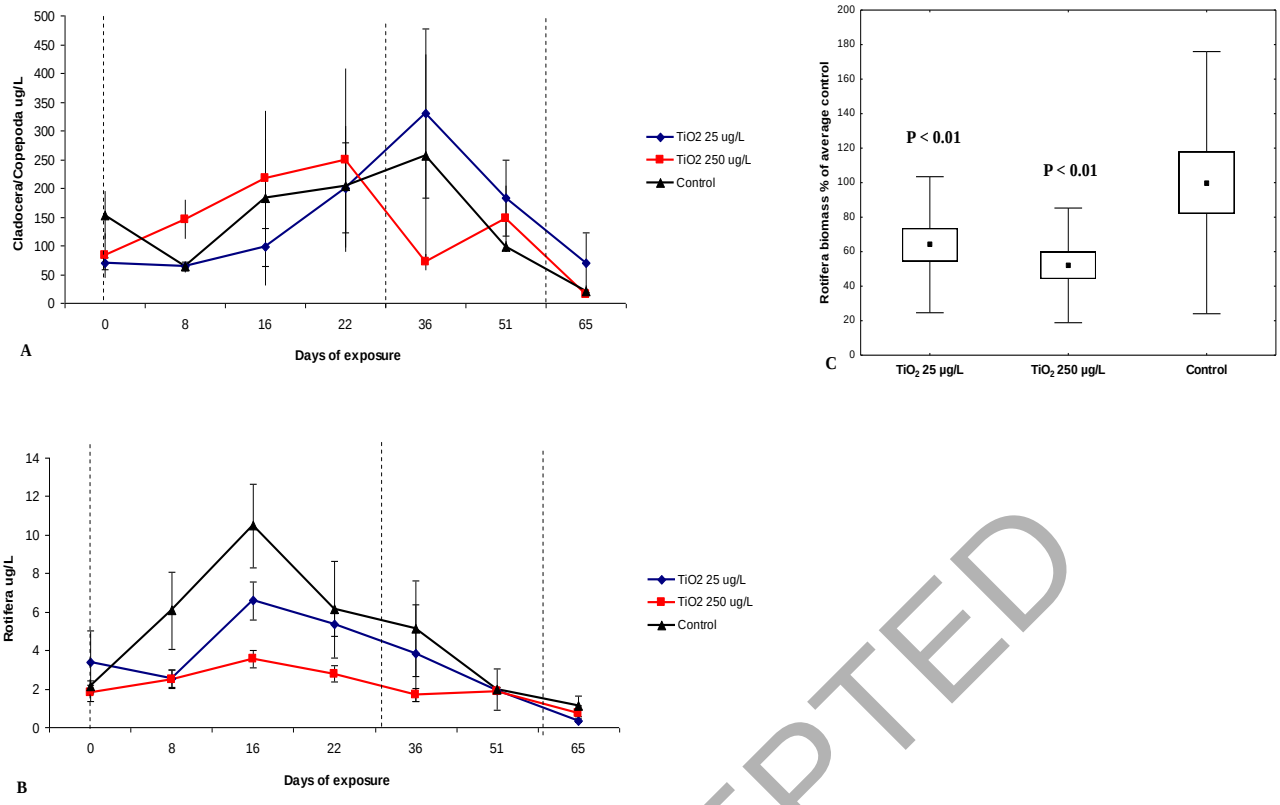

Figure 5

Table 1: Estimated average Hydrodynamic Diameter (d_H) of E171 TiO_2 over time. SD refers to standard deviation from 6 auto-repeated scans by the Malvern ZetaNano ZS.

Time	TiO_2 25 µg L^{-1} Lake Water **d_H (nm)** (mean ± SD)	TiO_2 25 µg L^{-1} Deionized Water **d_H (nm)** (mean ± SD)	TiO_2 250 µg L^{-1} Lake Water **d_H (nm)** (mean ± SD)	TiO_2 250 µg L^{-1} Deionized Water **d_H (nm)** (mean ± SD)
0 min	12550 ± 2	2494 ± 5	7110 ± 2	5540 ± 4
5 min	8488 ± 2	1796 ± 6	4414 ± 1	3622 ± 3
10 min	4199 ± 2	1635 ± 15	3266 ± 1	2991 ± 8
15 min	6489 ± 2	1513 ± 17	2033 ± 6	1744 ± 11
20 min	3915 ± 2	1441 ± 11	1411 ± 10	3058 ± 2
25 min	3740 ± 1	1150 ± 19	1532 ± 12	2791 ± 3
30 min	3532 ± 1	1320 ± 20	1421 ± 1	3974 ± 4
35 min	-	1545 ± 11	1261 ± 11	4168± 4
40 min	5980 ± 2	1457 ± 21	2655 ± 6	1943 ± 10
45 min	3920 ± 1	1112 ± 15	4271 ± 1	2135 ± 9
50 min	4261 ± 3	-	1154 ± 15	3817 ± 2
55 min	4895 ± 3	1282 ± 22	3195 ± 7	-
1 h	3319 ± 1	1296 ± 10	1636 ± 7	-
24 h	2415 ± 17	437 ± 54	433 ± 19	1148 ± 63

Table 2. Summary of all the measurements

	Before the start of the experiment (Day 0)						Throughout the experiment (Average of all samplings: Days 8-78)					
	Control		TiO_2 25 µg L^{-1}		TiO_2 250 µg L^{-1}		Control		TiO_2 25 µg L^{-1}		TiO_2 250 µg L^{-1}	
	Mean	SEM	Mean	SEM	Mean	SEM	Mean	SEM	Mean	SEM	Mean	SEM
TN mg L^{-1}	0.68	0.08	0.69	0.06	0.60	0.02	0.55	0.05	0.62	0.06	0.55	0.05
NO_2+NO_3 mg L^{-1}	0.01	0.00	0.01	0.00	0.01	0.00	0.01	0.00	0.02	0.00	0.01	0.00
NH_4^+-N mg L^{-1}	0.11	0.01	0.01	0.01	0.02	0.01	0.05	0.02	0.05	0.01	0.05	0.02
DIN mg L^{-1}	0.12	0.01	0.01	0.01	0.03	0.01	0.06	0.01	0.07	0.01	0.06	0.02
TP µg L^{-1}	31.78	2.33	32.88	2.80	29.41	2.69	45.59	4.38	46.97	3.34	41.36	4.21
SRP µg L^{-1}	6.22	0.14	6.34	0.34	5.69	0.23	7.96	1.13	6.82	0.80	6.14	1.03
Water temperature °C	16.95	0.03	16.89	0.01	16.91	0.01	21.35	0.35	21.38	0.35	21.19	0.34
Conductivity mS cm^{-1}	0.41	0.01	0.40	0.00	0.41	0.00	0.37	0.01	0.38	0.01	0.37	0.01
PAR light %*	-	-	-	-	-	-	35.74	1.47	36.57	1.58	40.45	1.72
Total suspended solids mg L^{-1}	25.75	2.72	25.35	3.52	41.45	22.67	32.26	6.13	30.91	5.50	28.11	6.10
Total dissolved solids g L^{-1}	0.27	0.00	0.26	0.00	0.27	0.00	0.24	0.01	0.25	0.01	0.24	0.01
Salinity g L^{-1}	0.20	0.01	0.19	0.01	0.20	0.00	0.18	0.01	0.18	0.01	0.18	0.01
O_2 mg L^{-1}	10.79	0.24	11.52	0.11	11.31	0.37	14.26	0.57	13.14	0.35	13.90	0.42
pH	8.40	0.01	8.39	0.06	8.35	0.08	8.68	0.12	8.55	0.10	8.65	0.11
Water column depth cm	89.33	0.66	88.67	1.33	88.67	1.33	80.24	1.41	82.67	1.31	82.38	1.26
Secchi depth cm	89.33	0.66	88.67	1.33	88.67	1.33	73.81	3.28	73.43	3.19	74.52	2.70
Chl-a µg L^{-1}	0.39	0.14	0.25	0.06	0.48	0.11	2.44	0.35	2.78	0.39	2.10	0.34
Periphyton wet biomass mg cm^{-2}	-	-	-	-	-	-	2.19	0.72	1.61	0.48	3.06	1.99
PVI %	-	-	-	-	-	-	47.91	10.11	46.12	9.61	45.21	8.58
Cladocera/Copepoda µg L^{-1}	153.72	42.38	69.13	10.06	83.07	39.78	137.52	41.37	157.59	34.96	141.18	32.69
Rotifera µg L^{-1}	2.12	0.32	3.37	1.63	1.79	0.41	5.16	1.18	3.52	0.67	2.19	0.25
	Before the start of the experiment (Day 0)						At the end of the experiment (Day 78)					
Chironomid biomass mg cm^{-2}	-	-	-	-	-	-	1.18	0.10	1.94	0.83	0.76	0.29
Fish biomass g m^3	≈9-10	-	≈9-10	-	≈9-10	-	10.79	1.25	9.74	0.83	8.80	0.09
P. pectinatus dry mass g	-	-	-	-	-	-	75.41	52.82	47.34	32.72	11.74	7.09
P. perfoliatus dry mass g	-	-	-	-	-	-	328.93	144.43	281.67	16.93	371.69	122.51

Chara sp. dry mass g	-	-	-	-	-	-	210.63	88.79	207.75	57.71	399.02	9.18
Najas sp. dry mass g	-	-	-	-	-	-	49.55	5.49	60.38	16.07	46.45	45.72
All macrophytes dry mass g	-	-	-	-	-	-	664.54	110.44	597.14	25.24	828.90	82.25

*These are average results for all measurements at the various water column depth